CARBON NANOTUBE COMPOSITE MICROACTUATORS: DESIGN AND CHARACTERIZATION

Pascal Hubert, Behnam Ashrafi, Kamal Adhikari, James Meredith, Srikar Vengallatore
McGill University, Department of Mechanical Engineering, 817 Sherbrooke Street West,
Montreal, QC, H3A 2K6, Canada

Keywords: *nanotubes, MEMS, nanocomposites, modelling, processing*

Abstract

Carbon nanotube-reinforced composites are a promising new class of structural materials for the mechanical components of microelectromechanical systems (MEMS). This paper presents an integrated design, manufacture, and characterization approach to the integration of nanocomposites within MEMS. The properties of nanocomposites are first analyzed by recourse to Eshelby-Mori-Tanaka theory. Subsequently, the processing and characterization of polymer-matrix nanocomposites are presented. Finally, the measurement of mechanical properties using nanoindentation-based methods is described. Implications of these results for the use of CNT nanocomposites in MEMS are discussed.

1 Introduction

Microactuators are the basic building blocks of microelectromechanical systems (MEMS) used for a wide variety of sensing and display applications. Typically, these actuators are simple beam or plate structures, with cross-sectional dimensions on the order of micrometers, and actuation is achieved by applying an electrical potential difference between the deformable structure and a fixed proximal electrode. The stiffness of the actuating structure dictates the force required for a specified deformation, and the natural frequency of vibration is a measure of the response time. Thus, many applications require the design of actuators with low stiffness and high natural frequencies of vibration. In terms of material selection, the stiffness and frequency are proportional to the Young's modulus and wave speed, respectively. Thus, the materials of choice for low-stiffness, high-frequency actuators should exhibit a combination of low modulus, E, and

high longitudinal wave velocity, $c = \sqrt{E/\rho}$, where ρ is the density.

The state-of-the-art in MEMS technology uses common ceramics (particularly silicon and silicon compounds) and metals (such as Al, Ni, Cu) as structural materials for actuators. In contrast, the use of fibre-reinforced composites has not been investigated, even though these materials exhibit an attractive combination of high wave speed and relatively low modulus. However, in order for a fibre to be used as reinforcement, the fibre diameter must necessarily be smaller than the cross sectional dimensions of the composite structure [1]. In this context, carbon nanotubes (CNT) emerge as attractive candidates for reinforcing microactuators because of their unique combination of small size and exceptional mechanical properties.

At the time of their discovery in 1991, carbon nanotubes were believed to be the ideal reinforcements for nanocomposites. Over the last decade, the research on synthesis and characterization of CNTs has produced a considerable literature on property values for CNT-polymer nanocomposites [1,2]. Much of the earlier work focused on the direct incorporation of the nanotubes as reinforcements in the resin. These resins were then processed to fabricate films, fibres, or bulk composites with enhanced mechanical and other multifunctional properties.

However, the global picture that emerges from this is discouraging – typically, the measured enhancements in properties are significantly less than expected. The difficulty of processing nanocomposites (especially in controlling alignment and dispersion, and in ensuring strong matrix-CNT interfaces) has been identified as a possible explanation. Processing of nanocomposites is a challenging task due in part to the effects of the nanotubes on the rheological and curing behaviour

PASCAL HUBERT, Behnam Ashrafi, Kamal Adhikari, James Meredith, Srikar Vengallatore

of the polymer. The viscosity of the matrix materials can increase by orders of magnitude upon the addition of carbon nanotubes due to their large aspect ratio (length/diameter > 500). The degree to which the viscosity is affected is highly dependent on the nanotubes type and aspect ratio [3], dispersion state [4] and functionalization [5]. Epoxy with functionalized nanotubes can exhibit a high degree of shear thinning behaviour compared to the neat resin [6]. Carbon nanotubes have been shown to affect the cure behaviour of resin systems as well. SWNT in epoxy act as strong catalysts even at low loadings of 5 wt% [7]. The presence of the nanotubes leads to an increase in the initial rate of reaction [8] and in the time to the maximum rate of reaction [9]. Thus, these effects cannot be ignored if one aims to have a full understanding of the processing of polymers in the presence of the nanotubes.

Here, we present an integrated design approach for the development of carbon nanotube-reinforced composite microactuators for MEMS. First, models based on computational micromechanics are used to predict the properties of nanocomposites. The effects of matrix properties and reinforcement characteristics (alignment, dispersion, volume fraction, and type of CNT) on elastic modulus and wave velocity are quantified. Subsequent sections discuss the processing of nanocomposite materials and their mechanical characterization using a custom-developed nanoindentation-based technique.

2 Theoretical Micromechanics

As a first step in evaluating the merits of CNT composites for microactuators, a detailed computational model was developed to predict the elastic properties of microactuator nanocomposite structures [10]. The Young's modulus is obtained as a function of the nanotube type, orientation, dispersion and volume fraction by using the Eshelby–Mori–Tanaka method. In this method, short fibres are approximated as ellipsoidal inclusions of aspect ratio $s = L/D$. With this assumption, the elastic constants can be calculated using the expression [10]:

$$\mathbf{C}^C = \mathbf{C}^M + V_f \left\langle \left(\mathbf{C}^N - \mathbf{C}^M \right) \mathbf{A}^N \right\rangle \left[\left(1 - V_f\right) \mathbf{I} + V_f \left\langle \mathbf{A}^N \right\rangle \right]^{-1} \tag{1}$$

where C^C, C^M, and C^N are the stiffness tensors of the composite, matrix, and nanotubes, respectively,

V_f is the nanotube volume fraction, I is the identity tensor, and terms enclosed in the angular brackets represent the average over all orientations. The dilute mechanical strain concentration tensor, A^N, is given by [10]:

$$\mathbf{A}^N = \left[\mathbf{I} + \mathbf{S} \left(\mathbf{C}^M \right)^{-1} \left(\mathbf{C}^N - \mathbf{C}^M \right) \right]^{-1} \tag{2}$$

where S is the Eshelby tensor whose components are functions of matrix Poisson's ratio and aspect ratio of the nanotubes. Expressions for the elements of S are listed elsewhere [10]. The nanotubes are assumed to be transversely-isotropic. Therefore, five independent elastic constants are required to describe the deformation of such structures. Elastic properties and density of three different types of carbon nanotubes, single-walled carbon nanotubes (SWNT), multi-walled carbon nanotubes (MWNT) and single-walled nanotube arrays, are listed in Table 1.

Table 1. Properties of nanotubes and nanotube-arrays [11,12].

	SWNT	MWNT	SWNT-array
E_{11}^N (GPa)	1060	800	580
E_{22}^N (GPa)	6.63	15.58	9.4
G_{12}^N (GPa)	442	320	17.2
G_{23}^N (GPa)	17	4.1	2.47
υ_{12}^N	0.16	0.14	0.18
ρ^N (kg/m^3)	1440	2090	1150

Fig. 1 shows the calculated Young's modulus for three different types of nanofibre reinforcements (SWNT, MWNT, and SWNT-array) in perfectly-aligned and perfectly-random orientations. The matrix material is a typical polymer with Young's modulus, Poisson's ratio, and density of 3.1 GPa, 0.4, and 1100 kg/m^3, respectively. In all cases, the aspect ratio of the nanotube and nanotube arrays is assumed to be 1000. The elastic modulus is observed to increase linearly with nanotube volume fraction, but the rate of increase is a function of the nanotube type and alignment. Aligned, dispersed SWNT are the most efficient reinforcements.
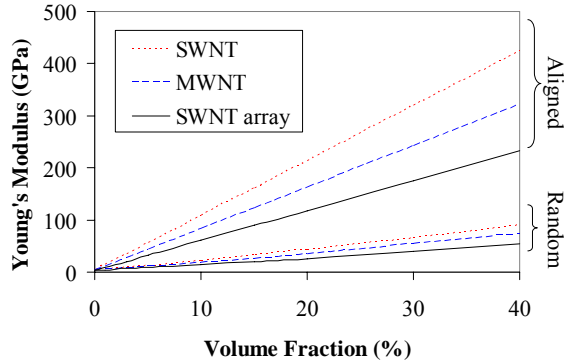
Fig. 1. Effect of reinforcement type, volume fraction, dispersion and alignment on composite Young's modulus

These results are then combined with a structural model based on Euler–Bernoulli beam theory to determine the longitudinal wave velocity of the nanocomposite beam (c^C):

$$c^C = \sqrt{\frac{E^C}{\rho^C}} \qquad (3)$$

Finally, the density of the nanocomposite (ρ^C) is calculated by the rule-of-mixtures:

$$\rho^C = (1 - V_f)\rho^M + V_f\rho^N \qquad (4)$$

where ρ^M and ρ^N are the densities of the matrix and nanotube, respectively.
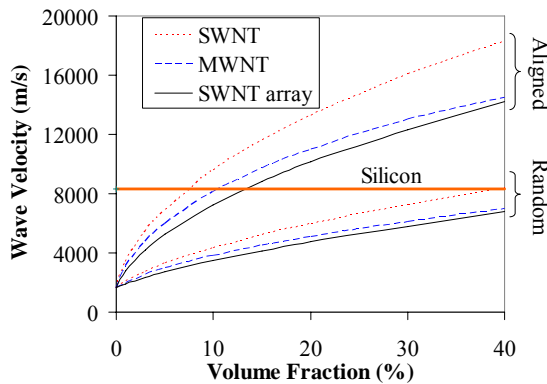

Fig. 2. Effect of reinforcement type, volume fraction, dispersion and alignment on the wave velocity of the composite beam.

The effects of nanotube volume fraction on the longitudinal wave velocity of the nanocomposite are shown in Fig. 2. As before, the matrix material is a typical polymer and, in all cases, the aspect ratio of the nanotube and nanotube arrays is 1000. The wave velocity is observed to be a non-linear function of volume fraction and the rate of increase is a function of the type of nanotube and alignment. The longitudinal wave velocity of monolithic silicon, a material widely used to manufacture microactuators, is also shown for comparison. Indeed, *at a carbon nanotube volume fraction of around 10%, the longitudinal wave velocity of the polymer-composite exceeds that of silicon.*

Representative curves are shown on a graph of wave velocity and Young's modulus (Fig. 3) for single-walled (SWNT) aligned polymer nanocomposites and multi-walled (MWNT) random nanocomposites. Also shown for comparison are the coordinates of monolithic metals (Au, Al, Ni) and ceramics (Si, SiC). The measured data for different polymer nanocomposites reported in the literature [2] is also plotted.
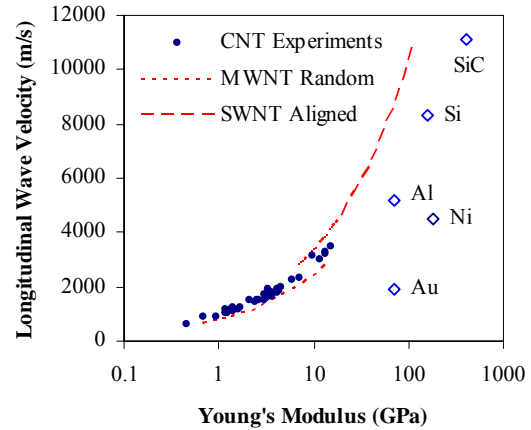

Fig. 3. Material selection chart for nanocomposite microactuators

Fig. 3 leads to the important observation that, under the ideal case, CNT polymer–matrix nanocomposites can attain longitudinal wave velocities comparable to metals and ceramics, but with significantly lower Young's modulus. Thus, these materials are ideal for electrostatic microactuators. However, there is an enormous gap between the state-of-the-art in nanocomposite technology and the nanocomposite characteristics required to match the properties of the monolithic ceramics and metals. Therefore, it is essential to undertake a systematic and thorough investigation of

the effects of processing parameters on mechanical properties of the CNT-polymer system.

3 Nanocomposites characterization

3.1 Materials

The nanotubes used for this work were functionalized single walled carbon nanotubes (f-SWNT) supplied by the National Research Council Canada's Steacie Institute for Molecular Sciences (NRC-SIMS) in Ottawa, Ontario, Canada. The nanotubes were prepared using a highly efficient laser-oven technique (Laser) and a proprietary high production throughput plasma process (Plasma). For the laser-oven technique, an inert environment of flowing Argon (250 sccm) was maintained inside a 45 mm diameter quartz tube fitted with a Brewster window. A gas-inlet was positioned at one end while a water-cooled collector and a pumping port was placed at the other. The quartz tube held a constant pressure of 500 Torr and a temperature of 1450 °C throughout the process. The graphite targets used were doped with 0.6 at% each of cobalt and nickel. Two types of lasers were used in this process. The first was a nanosecond-pulsed Nd:YAG laser (Spectra-Physics Pro290-30) operating at 1064 nm (or 532 nm) and 30 Hz with a fluence of approximately 2 Jcm^{-2}/pulse (and 1 Jcm^{-2}/pulse), respectively. This laser was setup for the purpose of vaporizing the graphite targets. The second laser, called the excitation laser, had the purpose of altering the rate of cooling of the condensing plume generated by the vaporizing laser. This laser was a Nd:YAG laser (Spectra-Physics Tornado S240-TN50-106Q) operating at either continuous wave or 20 kHz at a wavelength of 1064 nm and measured average powers of 50 and 48 W, respectively. The details of the production technique are given by Kingston et al. [13]. This production technique resulted in SWNT purity level reaching about 80 wt.% and metal catalyst contamination of under 6 wt.%. The remaining composition was made up of impurities such as amorphous and graphitic carbon particles. These nanotubes were then purified using a technique that is pending patent. Two types of functionalizations were applied to the nanotube structure: alkoxy and carboxyl groups were attached to the level of about 4 wt.%. The functional group was predicted to aid in the debundling and its homogeneous dispersion. For the nanotubes produced by the plasma process, only carboxyl functionalization was used (carboxyl USP).

The matrix used in this study was a standard aerospace grade epoxy, Araldite® MY0510 epoxy, supplied by Huntsman. This epoxy was used together with 4,4-Diaminodiphenyl Sulphone (DDS) as the hardener. The nanotube/epoxy mixture was prepared at NRC-SIMS by mixing 0.2 wt.% of SWNT in the MY0510 epoxy. In order to facilitate the mixing of the nanotubes in the resin, the MY510 was first dissolved in the organic solvent, Tetrahydrofuran (THF). The nanotubes were then dispersed using a highly efficient technique that is currently pending a patent. The THF was removed by placing the THF/f-SWNT/MY0510 in a near vacuum at 80°C for about 2.5 hrs until all the solvent had evaporated. Table 2 summarizes the material systems investigated in this work.

Table 2 Nanotube samples designation.

	Nanotube type
Alkoxy	Laser, purified
Carboxyl	Laser, purified
Carboxyl USP	Plasma, purified

3.2 Thermogravimetric characterization

Thermogravimetric analysis (TGA) indicates a structural modification of the epoxy system when subjected to a compatible nanotube functional group. The TGA tests were performed with a Perkin-Elmer TGA7 that was fully calibrated before performing any experiments. Three calibration routines had to be used in this process. First, a Furnace calibration was performed to match the thermocouple temperature and furnace temperature. This was followed by a Two-Standard calibration using nickel and iron to perform a Curie point calibration. Finally, the mass calibration of the TGA 7 was carried out using a 100mg standard.

The TGA experiments comprised of four sets of specimens: MY0510 (neat), MY0510/DDS, SWNT/MY0510 and SWNT/MY0510/DDS. In terms of the nanotube content, the SWNT/MY0510 had 0.2 wt.% of nanotubes while the SWNT/MY0510/DDS contained 0.125 wt.%. It was the addition of hardener in the case of the SWNT/MY0510/DDS in the recommended ratio (3 parts hardener to 5 parts resin) that led to a decrease in the weight percent of the nanotubes from 0.2 wt.% to 0.125 wt.%. While the MY0510 was poured into the sample holder as received, the MY0510/DDS, SWNT/MY0510 and

SWNT/MY0510/DDS resin was stirred manually using a glass stirrer for 30 mins before being poured into the sample holder to ensure homogeneity throughout. In order to prepare the other two samples, 25g of the respective resins were first stirred and poured into two separate sample holders followed by the addition of 15g of the hardener into each. This mixture was then manually stirred using a glass rod for a minimum of 30 minutes. Visually, the hardener appeared to dissolve after just 5 minutes of stirring; however, it was imperative to keep stirring the mixture to make sure that the distribution was homogeneous. The heating procedure for the TGA was specified using the software. In all the cases, the heating rate used was 20 ºC/min. The maximum temperature was 800 ºC and the sample was kept in air.

3.3 Rheological characterization

All the rheological experiments were conducted on a TAinstruments AR2000 rheometer with the Environmental Test Chamber (ETC) accessory. The measurement geometries used were 40 mm parallel aluminium plates cleaned with acetone. The geometry was then mapped by the rheometer along with its axial moment of inertia. A nominal value for the geometry was determined to be 2.65 ±0.02 μNms^2. The sample thickness between the parallel plates was kept in the range of 500 to 1000 μm (volume of 0.628 to 1.257 ml) per sample. This thickness was kept constant throughout the tests. Dynamic temperature tests (oscillatory temperature ramp) were performed on the nanocomposite mixture to observe the variations in the viscosity profile of the resins with temperature. The experiment was performed from room temperature to 250 ºC at a ramp rate of 3 ºC/min. The control variable of 12% strain was used with the sampling rate set at 1 point every 10 seconds. The post-experiment step set the temperature back to 25 ºC. The rheological experiments comprised of MY510/DDS and SWNT/MY0510/DDS samples.

3.4 Results

Fig. 4 presents the viscosity measured during cure as a function of temperature. The results clearly illustrated the effect of a dilute concentration of SWNT on the resin rheological behaviour. The plasma produced functionalized SWNT (Alkoxy and Carboxyl) increased the epoxy viscosity from an order of magnitude at room temperature (25°C) to almost two order of magnitude at 100°C for the carboxyl functionalization. For the alkoxy, a

reduction of the temperature of gelation of 10°C was observed. For the SWNT produced by plasma, the viscosity change with temperature follows closely the neat resin except between a temperature of 50-180°C. For these nanotubes, the viscosity profile is even lower than the neat resin between 50 and 180°C. This behaviour is presumed to be caused by the shorter length of the nanotubes produced by plasma compared to the laser process.

Fig. 5 shows the mass loss of the neat resin and epoxy/SWNT nanocomposites without curing agent (DDS) under air atmosphere. The SWNT affect the thermal degradation profile particularly after 350°C. This result indicates that the functionalized SWNT act as mild curing agents which react with epoxy groups. The alkoxy group has the best thermal stability followed by the USP carboxyl (plasma processed SWNT) and the carboxyl with the laser processed SWNT.
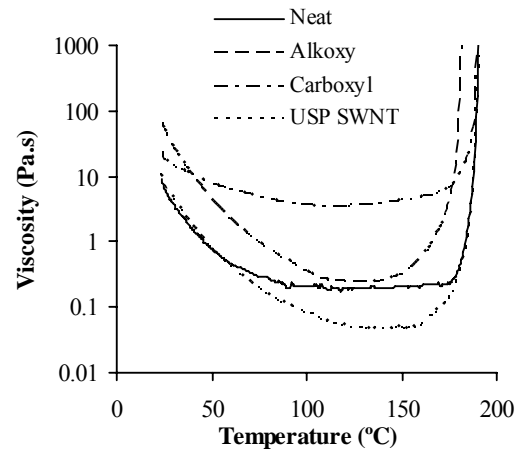

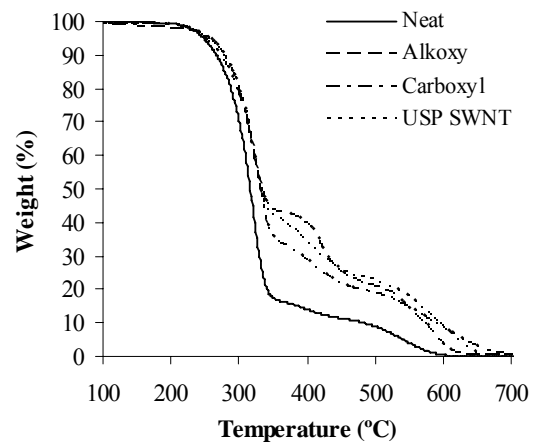Fig. 4. Viscosity profiles for 0.125% of SWNT in MY0510 and DDS curing agent.

Fig. 5. Weight loss for 0.2% of SWNT in MY0510 under air atmosphere.

Fig. 6 presents the thermal degradation profile of the neat resin and the SWNT/epoxy with the DDS curing agent. The neat resin profile without the curing agent is also shown for reference. These results confirm that the functionalized SWNT improved the thermal stability of the epoxy. Again, the alkoxy group lead to the best thermal stability compared to the carboxyl functionalization.
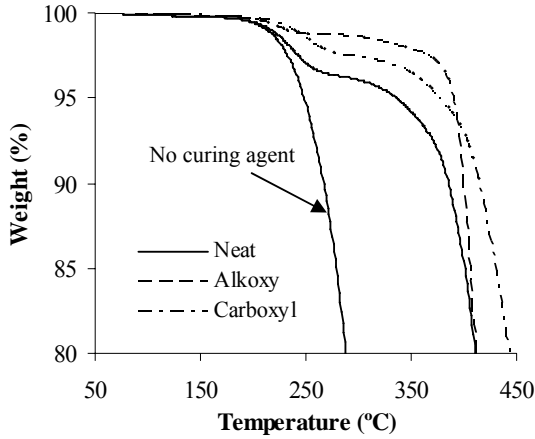

Fig. 6. Weight loss for 0.125% of SWNT in MY0510 and DDS curing agent under air atmosphere.

4 Elastic characterizations of soft thin films

Specimens for mechanical characterization were prepeared in the form of uniform thin films with thickness ranging from 25 to 200 μm. The films were cured between two glass substrates so as to obtain smooth surface finish (rms roughness <50 nm). Two different techniques were used to measure the Young's modulus of nanocomposite samples, namely, *nanoindentation* and *bending test*, as described below.

4.1 Nanoindentation

First, samples with a thickness exceeding 100μm were attached to a steel disk using superglue. Nanoindentation was performed using a commercial Hystiron Triboindenter with a Berkovich tip. The method of Oliver and Pharr was used to calculate the Young's modulus from the indentation load-displacement curves. In this technique, the slope of initial part of unloading curve is used to derive the contact stiffness (S_C), and the reduced Young's modulus is then calculated using [14]:

$$E_r = \beta \frac{2}{\sqrt{\pi}} \frac{\sqrt{A}}{S_C} \qquad (6)$$

Here, β is a constant that depends on the type of indenter ($\beta \approx 1$ for Berkovich tips) and A is the contact area. The reduced modulus is defined as:

$$\frac{1}{E_r} = \frac{1 - v_S^2}{E_S} + \frac{1 - v_I^2}{E_I} \qquad (7)$$

where E_s and v_s are Young's modulus and Poisson's ratio of the specimen, respectively. The corresponding properties of the indenter (E_I and v_I) are known: (for diamond tips, these values are 1000 GPa and 0.07, respectively). Hence, by combining Eqns. (6) and (7), and by assuming a value for the Poisson's ratio, it is possible to determine the Young's modulus of the specimen.

4.2 Bending test

In this method, the mechanical properties of thin films are measured using the bending of circular composite plate clamped at its edge. Fig. 7 shows a custom-made testing jig that is installed on a Hysitron Triboindenter to perform these tests. This instrument is capable of measuring loads and displacement with resolutions of a few μN and nm respectively. In addition, the Triboindenter is equipped with an optical system so that it is possible to specify the point of application of the load. The load-deflection curves obtained from the bending test, combined with a mechanical model for the bending deformation, are used to determine the Young's modulus of the specimen.

From Timoshenko's plate theory [15] the elastic Young's modulus of a clamped circular plate of radius a and thickness h is given by:

$$E = \frac{3(1 - v^2)}{4\pi} \frac{a^2}{h^3} \frac{P}{\delta} \qquad (8)$$

where P and δ are the load and deflection at the centre of the circular plate, respectively, and v is the Poisson's ratio of the film.
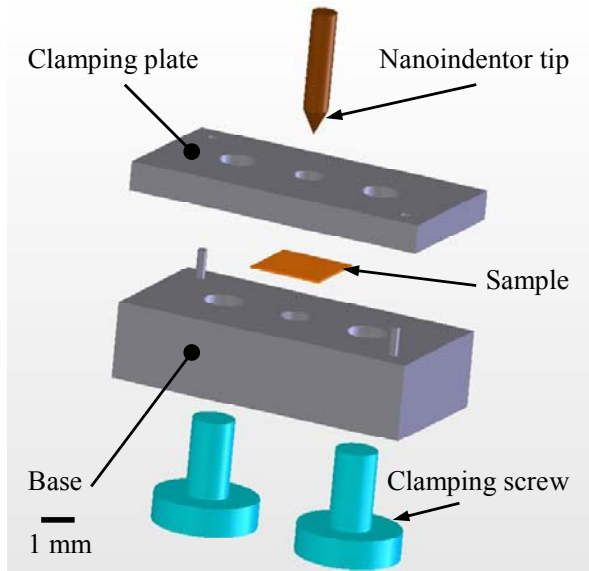
Fig. 7. Nanocomposite plate mechanical properties characterization fixture

The experimental protocol followed for the bending test is enumerated below.

1. The thickness of the film is obtained using a micrometer with a resolution of 1 μm.
2. The film is clamped between two plates and the centre of the film is located using the optical microscope in the Triboindenter.
3. A suitable load is applied at the center of the plate using a spherical indenter of radius 100μm, and the ratio of P/δ (i.e., the plate stiffness S_P) is measured from the load-deflection curve. Fig. 8 shows a typical load-displacement curve from a bending test.
4. Equation 8 is used to compute the Young's modulus from the slope of the load-deflection curve. The Poisson's ratio of the polymer is assumed to be 0.4 in these calculations.

4.3 Results

Table 3 lists the Young's modulus of a pure polymer (MY-0510 epoxy) and three different composites. The flexural modulus of MY-0510 epoxy is reported to be 3.4 GPa [16], which suggests that the bending method is more accurate than nanoindentation. This is expected since the Oliver-Pharr method used to interpret the nanoindentation data neglects the viscoelastic response of the polymer, and typically overestimates the elastic modulus of polymers [17,18].

Table 3 Elastic properties of MY-0510 polymer and their three different composites.

	E (GPa) Plate test	E (GPa) Indentation
Neat resin	3.4	4.2
Carboxyl	2.9	3.5
Carboxyl US	3.5	4.2
Alkoxy	3.5	4.2

By comparing the values of the pure polymer and the three different nanocomposites, we conclude that there is no significant enhancement of Young's modulus in these materials. Since the loading of CNT in these composites is small (<0.2 wt%), these values are consistent with expectations. Importantly, the above results demonstrate the establishment of a robust and reliable approach for the measurement of mechanical properties of small-volume specimens of nanocomposite materials.
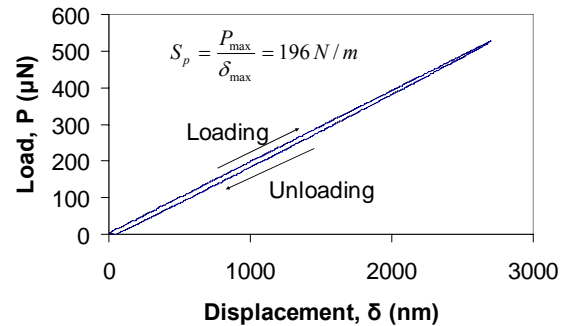

$$S_p = \frac{P_{max}}{\delta_{max}} = 196\,N/m$$

Fig. 8. Load-deflection curve for Carboxyl functionalized SWNT epoxy film with a thickness of 26 μm

5 Discussion and Conclusions

Microelectromechanical systems (MEMS) are being developed for applications ranging from information systems and communication to portable power generation and medicine. Enhancing the functionality, performance, reliability, and manufacturability of MEMS requires the integration of advanced nanomaterials with micromachining process flows. In that spirit, this work investigated the utility of carbon-nanotube-reinforced composites as structural materials for high-speed multifunctional microactuators. The nanocomposite structure was modeled as an isotropic matrix reinforced with transversely-isotropic carbon nanotubes. Three different types of nanotubes, namely, single-walled

carbon nanotubes (SWNT), multi-walled carbon nanotubes (MWNT), and arrays of single-walled carbon nanotubes (SWNT-array) were considered in the analysis. The elastic properties of the nanocomposite structure were analyzed by recourse to classical continuum mechanics within the framework of the Eshelby-Mori-Tanaka method, with the important assumption that the interfacial bonding between nanotubes and matrix is optimized for perfect load transfer.

The results indicate that reinforcement with carbon nanotubes enhances the axial Young's modulus and longitudinal wave velocity of nanocomposite beams. The extent of enhancement is a function of dispersion, alignment, aspect-ratio, and volume fraction of nanotubes, and the choice of matrix material. Furthermore, it is theoretically possible for polymers reinforced with aligned, high aspect-ratio, dispersed, single-walled carbon nanotubes to match the longitudinal wave velocities of common metals and ceramics. Thus, these nanocomposites are ideal candidates for low-force high-speed microactuators and for high-frequency micromechanical resonators.

The experimental thermal and rheological characterization of nanocomposites showed that the addition of functionalized SWNT has a significant effect on several intrinsic physical and chemical properties of the MY0510 epoxy. The degree to which the SWNT affects these properties is dependant on the type of functionalization. The effect of the nanotubes on the epoxy can be explained by the interaction of the nanotubes and its functional groups with the surrounding polymer. The results from this work suggest that the functionalized SWNT acts as a weak hardening agent and leads to a noticeable advancement of the epoxy. It is, thus, proposed that the alkoxy functional groups act as the reactive sites on the SWNT and bond with the surrounding polymer molecule. This leads to the formation of larger chains of polymers held "centrally" by the nanotubes. As such, part of the resin sample starts "polymerizing" prematurely leading to its advancement. This proposed mechanism is supported by some of the results of this work. The seven-fold increase of the viscosity of the MY0510 epoxy at room temperature in the presence of the alkoxy SWNT deserves a two-part interpretation. First, the addition of the high aspect ratio nanotubes has traditionally been shown to lead to an increase in the viscosity of the epoxy. In addition, the longer polymer chains that form as a result of the alkoxy

group tend to be less mobile and, thus, contribute to an increase in the viscosity of the MY0510. The role of the f-SWNT as a mild hardener is supported by the rheology data as well, where the epoxy starts gelling earlier, and at a lower temperature, in its presence. On the other hand, carboxyl functionalization of SWNT produced by plasma did not affect the viscosity profile of the epoxy. The lower nanotube aspect ratio compared to the SWNT produced by the laser process explains this behaviour.

Finally, the mechanical characterization of SWNT nanocomposite films was performed using nanoindentation and a microscale bending test. The results demonstrated the potential of this new technique for the accurate measurement of the elastic properties of nanocomposite thin films.

6 Acknowledgments

References

[1] Thostenson E.T., Li C. and Chou T.W., "Nanocomposites in context", *Composite Science and Technology*, 65, 491-516, 2005.

[2] Coleman J.N., Khan U., Blau W.J. and Gun'ko Y.K., "Small but strong: A review of the mechanical properties of carbon nanotube-polymer composites", *Carbon*, 44, pp. 1624-1652, 2006.

[3] Sung Y.T., Han M.S., Song K.H., Jung J.W., Lee H.S., Kum C.K., Joo J. and Kim W.N., "Rheological and electrical properties of polycarbonate/multi-walled carbon nanotube composites", *Polymer*, 47, 12, pp. 4434-4439, 2006.

[4] Kim J.A., Seong D.G., Kang T.J., Youn J.R., "Effects of surface modification on rheological and mechanical properties of CNT/epoxy composites", *Carbon*, 44, 10, pp. 1898-1905, 2006.

[5] Song Y.S. and Youn J.R., "Influence of dispersion states of carbon nanotubes on physical properties of epoxy nanocomposites", Carbon, 43, 77, pp. 1378-1385, 2005.

[6] Mitchell C.A., Bahr J.L., Arepalli S., Tour J.M. and Krishnamoorti R., "Dispersion of functionalized carbon nanotubes in polystyrene", *Macromolecules*, 35, 23, pp. 8825-8830, 2002.

[7] Puglia D., Valentini L. and Kenny J.M., "Analysis of the cure reaction of carbon nanotubes/epoxy resin composites through thermal analysis and Raman spectroscopy", *Journal of Applied Polymer Science*, 88, 2, pp. 452-458, 2003.

[8] Xie H., Liu B., Yuan Z., Shen J. and Cheng R., "Cure kinetics of carbon nanotube/tetrafunctional epoxy nanocomposites by isothermal differential scanning calorimetry", *Journal of Polymer Science: Part B: Polymer Physics*, 42, 20, pp. 3701-3712, 2004.

[9] Wang S., Liang Z., Liu T., Wang B. and Zhang C., "Effective amino-functionalization of carbon nanotubes for reinforcing epoxy polymer composites", *Nanotechnology*, 17, 6, pp. 1551-1557, 2006.

[10] Ashrafi B., Hubert P. and Vengallatore S. "Carbon nanotube-reinforced composites as structural materials for microactuators in microelectoromechanical systems". *Nanotechnology*, 17, pp. 4895-4903, 2006.

[11] Shen L. and Li J. "Transversely isotropic elastic properties of single-walled carbon nanotubes" *Physical Review B*, 69, 045414, 2004.

[12] Ashrafi B. and Hubert P. "Modeling the elastic properties of carbon nanotube array/polymer composites". *Composites Science and* Technology, 66, pp. 387–396, 2006.

[13] Kingston C.T., Jakubek Z.J., Dénommée S. and Simard B., "Efficient laser synthesis of single-walled carbon nanotubes through laser heating of the condensing vaporization plume", *Carbon*, 42(8-9): pp. 1657-1664, 2004.

[14] Oliver W.C. and Pharr G.M., "Measurement of hardness and elastic modulus by instrumented indentation: Advances in understanding and refinements to methodology". *J. of Materials Research*, 19, pp. 3-20, 2004.

[15] Timoshenko S., "Theory of plates and shells". 2nd edition, McGraw-Hill, 1959.

[16] Araldite® MY 0510+DDS data sheet by Huntsman.

[17] Vanlandingham M.R., Villarubia J.S., Guthrie W.F. and Meyers G.F., "Nanoindentation of polymers: an overview", *Macromolecule Symposium*, 169, pp. 15-43, 2001.

[18] Tranchida D., Piccarolo S., Loos J., and Alexeev A., "Accurately evaluating the Young's modulus of polymers through nanoindentation: A phenomenological correction factor to the Oliver and Pharr procedure", *Appl. Phys. Lett.*, 89, 171905, 2006